© 2021. Published by The Company of Biologists Ltd | Journal of Experimental Biology (2021) 224, jeb242694. doi:10.1242/jeb.242694

RESEARCH ARTICLE

Plasticity of the gastrocnemius elastic system in response to decreased work and power demand during growth

Suzanne M. Cox[1,2,*], Adam DeBoef[2,3], Matthew Q. Salzano[2,4,5], Kavya Katugam[2], Stephen J. Piazza[2] and Jonas Rubenson[2,4]

ABSTRACT

Elastic energy storage and release can enhance performance that would otherwise be limited by the force–velocity constraints of muscle. Although functional influence of a biological spring depends on tuning between components of an elastic system (the muscle, spring-driven mass and lever system), we do not know whether elastic systems systematically adapt to functional demand. To test whether altering work and power generation during maturation alters the morphology of an elastic system, we prevented growing guinea fowl (*Numida meleagris*) from jumping. We compared the jump performance of our treatment group at maturity with that of controls and measured the morphology of the gastrocnemius elastic system. We found that restricted birds jumped with lower jump power and work, yet there were no significant between-group differences in the components of the elastic system. Further, subject-specific models revealed no difference in energy storage capacity between groups, though energy storage was most sensitive to variations in muscle properties (most significantly operating length and least dependent on tendon stiffness). We conclude that the gastrocnemius elastic system in the guinea fowl displays little to no plastic response to decreased demand during growth and hypothesize that neural plasticity may explain performance variation.

KEY WORDS: Ontogeny, *Numida meleagris*, Morphology, Musculoskeletal modeling, Guinea fowl

INTRODUCTION

Taking advantage of storage and release of elastic strain energy can enhance performance that would otherwise be limited by the force–velocity constraints of muscle. The temporal decoupling of energy production from energy delivery permitted by elastic energy storage allows muscles and tendons to produce force effectively over a wider range of shortening or lengthening speeds. Muscles may generate forces during slow or isometric contractions while elastic recoil augments the rate of energy delivery or absorption during rapid movements (Patek et al., 2011; Roberts and Azizi, 2011). By making use of energy storage in the tendon 'spring', a muscle–tendon unit (MTU) can produce force more economically or with greater power than a muscle alone (Roberts and Azizi, 2011). Yet, several studies have identified important differences among spring–muscle combinations. Wilson, Lichwark and colleagues (Lichtwark and Wilson, 2008; Wilson et al., 2000) showed that the efficiency of an MTU during cyclic loading depends on the tuning of relative muscle and spring properties. For instance, muscle efficiency varies with both fascicle length and tendon stiffness, with the specific optimal efficiency values depending on gait conditions (Lichtwark and Wilson, 2008). Several researchers (Astley and Roberts, 2012, 2014; Galantis and Woledge, 2003; Ilton et al., 2018; Richards and Sawicki, 2012) have shown that the opposing inertial or drag forces acting on a motor–spring system also influence whether springs enhance performance. Adding further complexity, several studies (Robertson and Sawicki, 2014; Robertson et al., 2018; Sawicki et al., 2015) have found that the timing of neural activation of muscle must be tightly controlled to take advantage of in-series springs. Together, this body of work suggests that understanding the conditions in which spring systems enhance performance may require expanding our focus from the MTU to that of the broader 'elastic system' that includes the muscle (motor), the spring, the resistive forces and the neural control of the system. The optimal performance of an elastic system may require tuning of both morphology and neural control. This approach recognizes the integrated nature of the neuro-musculoskeletal system (Nishikawa et al., 2007).

The sensitivity of elastic system efficiency to the tuning of its components complicates inferences for how elastic systems systematically adapt to functional demand during maturation. For instance, do growing individuals who regularly perform functions that utilize elastic strain energy develop elastic systems with greater energy storage capacity? This is still unknown because most studies of MTU plasticity have focused on how individual components of elastic systems [neural control (Gillis and Biewener, 2001; Kao et al., 2010; Lutz and Rome, 1996), muscle (Du and Standen, 2017; Estes et al., 2017; Minamoto et al., 2015; Lieber et al., 2017) and tendon (Bohm et al., 2014; Bohm et al., 2019; Docking and Cook, 2019; Eliasson et al., 2007; Katugam et al., 2020; Kubo et al., 2007)] vary with task or training, and how those individual changes influence function of an MTU (Albracht and Arampatzis, 2006; Mayfield et al., 2016; Robertson and Sawicki, 2014; Rosario et al., 2016; Sawicki et al., 2015). Yet, the integrated nature of the elastic system suggests that functional consequences of plasticity are difficult to predict by analyzing elements in isolation (Albracht and Arampatzis, 2006; Ettema, 1996; Zajac, 1992). Therefore, the complex nature of the neuromuscular adaptation of elastic systems may require analysis at the system level rather than at the level of individual components.

Here, we present a study of the morphological plasticity of an elastic system. Specifically, we ask whether individuals that jump

[1]Biology Department, Duke University, Durham, NC 27708, USA. [2]Biomechanics Laboratory, Department of Kinesiology, The Pennsylvania State University, University Park, PA 16802, USA. [3]The Department of Biological Sciences, Georgia Institute of Technology, Atlanta, GA 30332, USA. [4]Integrative and Biomedical Physiology, The Pennsylvania State University, University Park, PA 16802, USA. [5]Department of Kinesiology, The University of Massachusetts, Amherst, Amherst, MA 01003, USA.

*Author for correspondence (smc69@duke.edu)

S.M.C., 0000-0002-9704-0716; A.D., 0000-0003-1446-5151; M.Q.S., 0000-0003-4000-982X; S.J.P., 0000-0002-5026-7569; J.R., 0000-0003-2854-1776

Received 12 April 2021; Accepted 8 September 2021

Journal of Experimental Biology (2021) 224, jeb242694. doi:10.1242/jeb.242694

during maturation (an activity requiring elastic energy storage and return; Henry et al., 2005) develop elastic systems that are more capable of storing elastic strain energy at maturity than those of individuals restricted from jumping. We focus on the elastic system most involved in storage and release of elastic energy during jumping (Alexander, 1968; Arellano et al., 2019; Biewener et al., 2004; Farris et al., 2016; Walmsley et al., 1978), the gastrocnemius elastic system. We test this by altering the rearing conditions of two groups of guinea fowl (*Numida meleagris*) across the entire growth period, allowing one group to engage in jump-to-perch behavior and preventing all jumping in the other group. Guinea fowl are a particularly good species with which to study these questions because they generate peak powers three times greater than possible with muscle alone during jumping, producing forces over six times their body weight (Katugam et al., 2020), which suggests that energy storage and release are particularly important to their jump performance (Roberts and Hoppeler, 2016). We previously reported that restricted birds in another portion of this study showed detriments in jump performance at adulthood (Cox et al., 2020). In this paper, we aim to link the morphological and functional consequences of our intervention.

In analyzing the morphology data, we took both an individual-component and a systems-level approach to evaluate the plasticity of an elastic system during growth. At the component level, we probed whether our treatment resulted in systematic morphological differences in individual components of the gastrocnemius elastic system between groups. We sought to determine whether components of this elastic system plastically adapt to variations in functional demand during growth. At the systems level, we asked how plastic changes at the component level interact to influence the capacity for elastic energy storage. To do this, we developed subject-specific musculoskeletal models that incorporated experimentally measured morphological properties of each bird's elastic system. With each subject-specific model, we simulated a fully activated muscle contraction under various postures and quantified the resulting tendon strain energy stored. The purpose of this systems-level analysis was to evaluate the integrated effects of morphological variation on the limits of energy storage capacity of each bird.

The component- and systems-level analyses serve as a case study for understanding how a particular elastic system changes with functional demand. We also took advantage of the variation within and across groups to ask broader questions about the relationship between form and function in elastic systems. Specifically, we asked which combinations of naturally occurring morphological variation most influence the ability of an elastic system to store energy. Lastly, because the elastic system requires tuning of both morphology and neural control and energy storage capacity is only one piece of the puzzle, we tested whether jump performance is constrained by the limits of energy storage capacity. Specifically, we asked whether birds with lower energy storage capacity produce less work and power during jumping.

We hypothesized that components of an elastic system plastically adapt to variations in functional demand during maturation, resulting in greater energy storage capacity in birds that jump during growth. We predicted that energy storage capacity would increase linearly with muscle force-generating capacity and inversely with tendon stiffness (Biewener and Baudinette, 1995; Biewener and Roberts, 2000; Kubo et al., 1999). Finally, we predicted that differences in jump performance would positively correlate with an animal's ability to store elastic strain energy in the tendon of the gastrocnemius elastic system.

MATERIALS AND METHODS

Experimental protocol

Animals

To study these questions, 1-day-old guinea fowl [*Numida meleagris* (Linnaeus 1758)] keets were obtained from a regional breeder (Guinea Farm, New Vienna, IA, USA). After a 2-week brooding period, the keets were pen reared through skeletal maturity (>6 months) in one of two conditions, as we previously described in detail (Cox et al., 2020). A control group (C; n=8) was housed in a large, circular pen (3.14 m^2) that allowed ample room for locomotion and objects for jumping and perching. The restricted treatment group (R; n=7) was raised in a smaller pen (1 m^2 at maturity) with low mesh ceilings that prevented jumping. Food and water were available *ad libitum* (food intake did not differ between groups). Lights were programmed to be on a 12 h:12 h light:dark cycle. This protocol resulted in no changes in time spent walking or standing between groups, but drastically altered the average number of jumps per day. The control group jumped twice their body height, on average, 194 times a day, whereas the restricted birds were restricted from jumping entirely (Cox et al., 2019a). The experimental protocol was approved by the Institutional Animal Care and Use Committee at The Pennsylvania State University (ref. 46435)

Functional measures

As described previously (Cox et al., 2020), at skeletal maturity (between 29 and 31 weeks old) jump performance was measured by placing each bird in turn on 6×6 inch (15.24×15.24 cm) force plates (AMTI HE6x6; Watertown, MA, USA) enclosed in a tapered box and encouraging the birds to jump. Jump power was calculated from the instantaneous net vertical ground reaction and the vertical center of mass velocity. The horizontal component of GRF was ignored because the experimental setup constrained jumps to be nearly vertical. Velocity was obtained by integrating the center of mass acceleration, which was in turn found from the net ground reaction force and the body mass. We calculated jump work by integrating the instantaneous power with respect to time over the course of the jump. At the end of functional data collection, birds were euthanized (intravenous pentobarbital, >160 mg kg^{-1}).

Quantification of properties of individual components of the elastic system

Specimen muscle architecture preparation

The pelvic limb was separated from the upper body and the left and right legs were then split by sectioning the pelvis at the midline while avoiding muscle attachments. Right limbs were placed into neutral buffered formalin for fixation (10%) for at least 2 weeks, while left legs were fresh-frozen and kept at −20°C. Right limbs were positioned with joint angles approximating those at mid-swing during running [hip: 30 deg; knee: 80 deg; ankle: 125 deg; within ±2 deg (Rubenson and Marsh, 2009)]. Joint angles were confirmed for the fixed limbs using photographs made with a digital camera (Canon EOS550D; Surrey, UK) and analyzed with ImageJ (National Institutes of Health, Bethesda, MD, USA).

Muscle analyses

We made measurements of the lateral and medial heads of the gastrocnemius muscle (LG and MG, respectively), the muscle group of the MTU thought primarily responsible for storage and release of elastic strain energy during running and jumping (Arellano et al., 2019; Henry et al., 2005). The third (intermedia) head of the gastrocnemius only comprises ∼10% of the total mass of the gastrocnemius muscles in this species (Rubenson et al., 2006) and

Journal of Experimental Biology (2021) 224, jeb242694. doi:10.1242/jeb.242694

thus was not included in the analysis. MG and LG were dissected from the fresh-frozen left limbs and weighed to the nearest 0.1 mg. The LG and MG were then dissected from the fixed limbs for fascicle length, pennation angle and sarcomere analysis. The LG was first split longitudinally through the mid-belly to view fascicle arrangement. Photographs of whole MG and split LG made with a digital camera (Canon EOS550D with Canon EFS 18-55 and 10× lens) were imported into ImageJ for measurement of the pennation angle between muscle fascicles and their insertions on the aponeurosis (Salzano et al., 2018).

Owing to the expected within-muscle heterogeneity of strain (Ahn et al., 2003; Azizi and Deslauriers, 2014), each muscle was divided into sections for analysis. The MG was split into anterior and posterior fascicles (Carr et al., 2011) and then further split into proximal and distal fascicles, resulting in four sections. The LG was split into proximal, middle and distal sections, each spanning one-third the length of the muscle belly. Average pennation angle was found for each section by taking the mean of three angle measurements. Sarcomere lengths for each section were found using the laser diffraction techniques described in Salzano et al. (2018). A minimum of three sarcomere length measurements were taken from each muscle fascicle bundle and these measurements were averaged to obtain the mean measured sarcomere length.

Optimal fascicle length, L_O, was calculated by multiplying the length of the fascicle by the ratio of optimal sarcomere length of guinea fowl muscle (2.36 µm; Carr et al., 2011) to the mean measured sarcomere length.

Pennation angle at optimal fascicle length (θ_{OFL}) was calculated from the average measured pennation angle ($\bar{\theta}$) and the ratio of measured fiber length (L_F) to the calculated optimal fiber length (L_O) according to the equation (Buchanan et al., 2004):

$$\theta_{OFL} = \sin^{-1}\left\{\frac{L_F \sin\bar{\theta}}{L_O}\right\}. \quad (1)$$

Maximum isometric force along the muscle fiber for the MG and LG was approximated from the muscle mass (m), L_O and muscle density (ρ_{musc}=1060 kg m^{-3}; Mendez and Keys, 1960) using the specific tension (f, 3×10^5 N m^{-2}; Rospars and Meyer-Vernet, 2016), according to the equation:

$$F_{max} = \frac{fm}{\rho_{musc} L_O}. \quad (2)$$

We specifically calculated isometric force along the muscle fiber for input into the musculoskeletal model rather than including the influence of pennation angle because pennation angle is a separate input into the OpenSim Millard muscle model (see below for model description), which accounts for the change in pennation angle with muscle length (Millard et al., 2013).

Moment arm

The gastrocnemius moment arm at the ankle was experimentally measured using the tendon travel method (Landsmeer, 1961; Spoor and van Leeuwen, 1992) as described by Salzano (2020). In short, the Achilles tendon (which attaches only to the LG, MG and IG in guinea fowl) was attached to a linear transducer (model P510-2-S11-N0S-10C, UniMeasure, Corvallis, OR, USA) to measure excursion and kept at a constant 10 N tension to prevent changes in tendon strain (Fig. 1). Retroreflective markers were placed on dissected limbs to track the relative movement of the tibia and tarsometatarsus in 3D across a range of joint angles using a four-camera motion analysis system (300 Hz; Kestrel, Motion Analysis Corporation, Santa Rosa, CA, USA), and automatically synchronized to the linear transducer data within the motion analysis software (Cortex, Motion Analysis Corporation). Joint centers and a mean helical axis were calculated from motion data for each trial and used to calculate flexion angle at the ankle at each time point (Lewis et al., 2006). A cubic spline was fit to the tendon excursion versus flexion angle points using least-squares approximation, and tendon excursion was differentiated with respect to angle to estimate moment arm across the measured range of motion (30–90 deg). Average values are reported in Table 1.

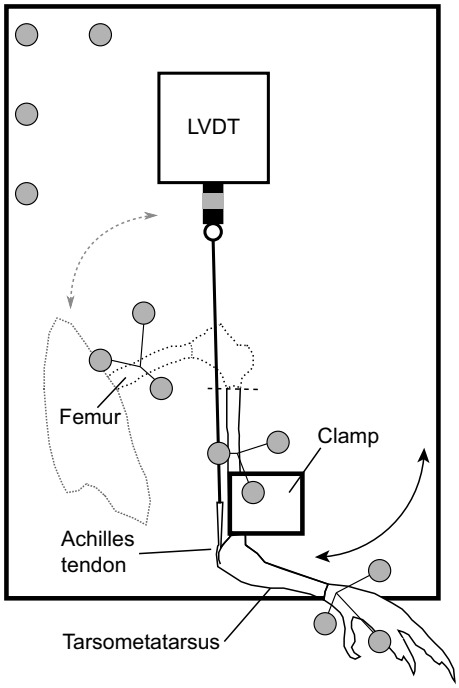

Fig. 1. Setup for the tendon travel experiment. The limb was positioned so that the tibiotarsus was held firm by a 3D printed clamp. In the knee joint motion trial, the femur was rotated to move the knee through its range of motion. The tibiotarsus was then cut to remove the proximal portion of the limb, allowing for the LVDT to be attached to the Achilles tendon. For tendon travel trials, the tarsometatarsus was rotated to move the ankle through its range of motion. Gray coloring represents retroreflective markers on the limb and linear variable differential transformer (LVDT). The dotted line outlines the pelvis femur and knee, which were removed after the knee joint motion trial. The dashed line represents location at which the tibiotarsus was cut after the knee joint motion trial. Figure adapted from Salzano (2020).

Tendon force–length curves

We quantified the tendon force–length properties with material analysis as described in Katugam et al. (2020). In short, tendons were detached from the gastrocnemius muscles but left attached at their insertion points on the tarsometatarsus bone. Both the bone and the tendon's proximal end were connected to a material testing machine (858 Mini Bionix II; MTS Systems, Eden Prairie, MN, USA). Samples were mounted vertically using custom clamps on the tendon aponeurosis and the tarsometatarsus and attached to a 50-pound load cell (MTS Systems). The upper clamp gripped the entire aponeurosis of each sample, leaving only the free tendon exposed to loading. The tendon force–length properties were quantified by loading the tendon cyclically (20 cycles) to 4% strain. The tendon force–length curves were calculated by averaging the data from last 5 cycles of the loading protocol. Tendon force–strain curves were calculated by normalizing displacement by the length of the tendon (T_L) measured to the

Journal of Experimental Biology (2021) 224, jeb242694. doi:10.1242/jeb.242694

Table 1. Morphological and functional measures by treatment

	Restricted	Control	*P*
Total animals	8	8	
Body mass (kg)	1.7 (0.11)	1.7 (0.14)	0.5
Extensor muscle mass (kg)	0.239 (0.022)	0.257 (0.02)	0.18
Average moment arm (cm)	0.91 (0.05)	0.94 (0.03)	0.24
Tendon stiffness (kN m^{-1})	48.1 (13)	53.5 (10)	0.39
Leg length (mm)	345 (11)	349 (18)	0.56
Femur length/leg length	0.25 (0.01)	0.25 (0.01)	0.18
Tibia length/leg length	0.36 (0.01)	0.35 (0.01)	0.1
Tarsometatarsus length/leg length	0.22 (0.01)	0.22 (0.01)	0.55
Toe length/leg length	0.17 (0.01)	0.17 (0.01)	0.63
At maturity*			
Max. jump take-off velocity (m s^{-1})	**3.3 (0.43)**	**4.0 (0.36)**	**0.007**
Jump work (J kg^{-1})	**37 (9.2)**	**50 (8.4)**	**0.013**
Peak power (W kg^{-1})	**787 (165)**	**1171 (117)**	**3.5e–4**
Peak jump force/body weight (N N^{-1})	**4.7 (0.54)**	**6.7 (0.74)**	**5e–5**

All values are given as means±s.d. *P*-values are shown for statistical comparisons between groups. Bolded rows show statistically significant differences between groups. *Data reproduced from Cox et al. (2020).

Table 2. Muscle morphological data by treatment for the lateral (LG) and medial (MG) gastrocnemius muscles

	Restricted	Control	*P*
LG			
Muscle mass (g)	9.0 (1.3)	9.2 (1.5)	0.77
Optimal fiber length (mm)	24 (2.9)	24 (4.1)	0.95
Max. isometric force (N)	105 (15)	110 (22)	0.64
Pennation angle (rad)	0.33 (0.05)	0.30 (0.07)	0.38
Tendon slack length (mm)	135 (7.3)	139 (6.5)	0.32
MG			
Muscle mass (g)	11 (1.4)	12 (1.8)	0.2
Optimal fiber length (mm)	28 (4.2)	29 (3.5)	0.81
Max. isometric force (N)	108 (20)	118 (29)	0.44
Pennation angle (rad)	0.20 (0.03)	0.21 (0.03)	0.51
Tendon slack length (mm)	150 (8.3)	150 (9.1)	0.97

Morphological measures did not vary between groups. All values are given as means±s.d. *P*-values are shown for statistical comparisons between groups. Muscle pennation angle is at optimal fiber length.

nearest 0.1 mm with calipers while under zero force in the material testing setup. Average values for tendon stiffness given in Table 1 were calculated from the slope of the tendon force–length curve across the last 50 points measured in the last 5 cycles of trials, at strain between 3 and 5%.

Tendon slack length

The tendon slack lengths for the LG and MG were estimated from experimental measures as described in the Supplemental Materials & Methods. Because model based estimates of muscle fiber length in a given posture are particularly sensitive to the tendon slack length (Ackland et al., 2012; De Groote et al., 2010; Scovil and Ronsky, 2006) and our calculations involved several simplifying assumptions, we further refined our experimental estimates of tendon slack length by fine-tuning the tendon slack length parameter in the OpenSim model (see Supplemental Materials & Methods for experimental tendon slack length measurement, and see below and Supplemental Materials & Methods for model development). After experimental moment arms and tendon and muscle properties were added to subject-specific models, each model was posed in the individual's fixed posture. The model's tendon slack length was adjusted iteratively in the model until the LG and MG normalized fiber lengths were within 1% of the experimentally measured values. These final values are listed in Table 2.

Quantifying the influence of restricted jumping on energy storage capacity

We generated a flock of subject-specific musculoskeletal models by modifying the generic model (Cox et al., 2019b) to match experimental values measured for each bird (see Supplemental Materials & Methods). With these models, we quantified the capacity of each subject-specific model to store elastic energy in its Achilles tendon across a range of joint postures (ankle: 31 to 145 deg, knee: −145 to −15 deg; Fig. 2) (Cox et al., 2019b). At each posture, the simulated LG and MG were activated at 100% and the MTU was equilibrated with the OpenSim MATLAB equilibrateMuscles() function, which adjusts muscle and tendon length such that tendon force and muscle (active and passive) forces balance. The LG and MG insert on the same tendon but, because of OpenSim modeling constraints, these muscles are modeled as having separate tendons. To calculate the stored elastic energy in the combined Achilles tendon, then, we first extracted the resulting force (f_a) along the tendon for each muscle. These values were summed and the resulting tendon strain in a single tendon (ε_{Ta}) was found from the inverse of the experimentally measured force–strain curve:

$$\varepsilon_{Ta} = \boldsymbol{g}^{-1}(f_a). \quad (3)$$

The strain energy stored in the strain of the tendon (PE; Eqn 4) was calculated by integrating the tendon force–strain curve from zero to the calculated strain and multiplying that by the tendon sample length (L_T) as measured at zero strain during the material testing:

$$PE = L_T \int_0^{\varepsilon_{Ta}} \boldsymbol{g}(\varepsilon)\mathrm{d}\varepsilon. \quad (4)$$

Simulations of 100% activation of the LG and MG were performed across the range of experimentally measured joint angles for the ankle and knee joint (Fig. 2A,B). From these simulations, we extracted the maximum elastic energy storage across all postures for each bird and the ankle and knee angles at which the maximum was achieved, and recorded the values in a pre-jump posture (Fig. 2C) (Henry et al., 2005). Tendon elastic energy stored in the pre-jump posture has been found to be a requirement for the very high power generated in guinea fowl jumping (Cox et al., 2020; Henry et al., 2005). Additionally, we recorded the normalized fiber length for each muscle at this posture at zero activation.

Statistical tests

To determine whether components of the gastrocnemius elastic system change systematically in response to changes in demand, we evaluated the influence of treatment group (restricted versus control) on each element of morphology measured. This was accomplished using *t*-tests if the homogeneity of variance assumption test was passed, and using a Kruskal–Wallis test by ranks when this criterion was not met. The threshold for statistical significance was set at 0.005 after a Bonferroni correction for multiple comparisons. Likewise, the relationship between treatment group and elastic energy storage capacity was

Journal of Experimental Biology (2021) 224, jeb242694. doi:10.1242/jeb.242694

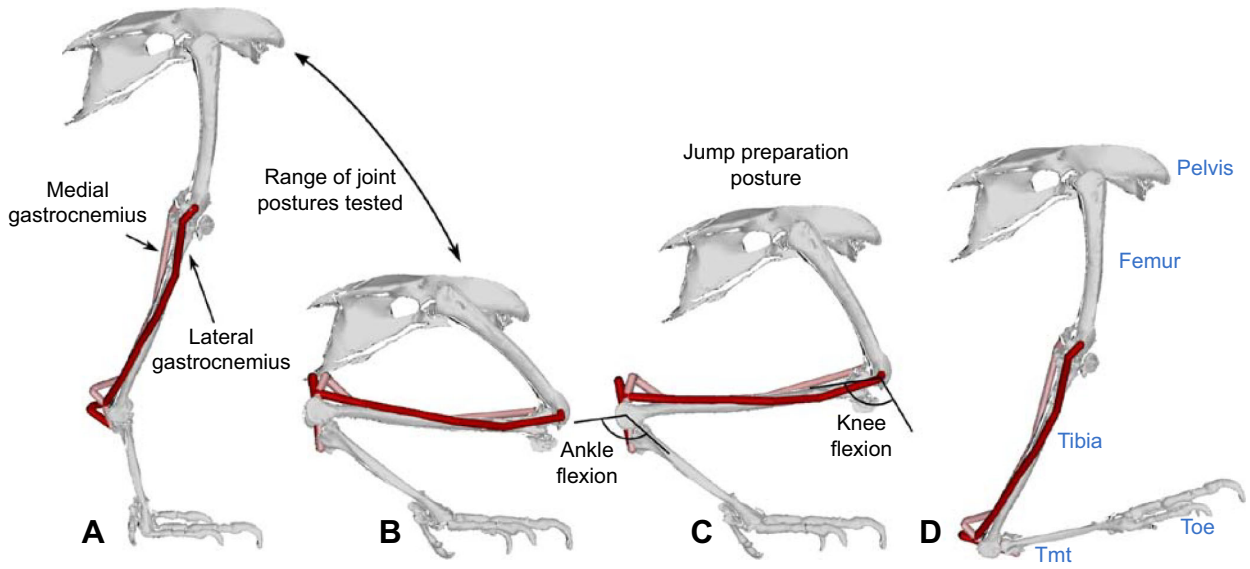

Fig. 2. Illustrations of joint postures utilized in this study. Elastic energy storage potential was evaluated across a range of experimentally observed joint postures (A,B). The average posture guinea fowl take in preparation for a jump (C) has a much more flexed knee than the optimal posture for energy storage (D). Tmt, tarsometatarsus.

evaluated with a *t*-test after data passed tests for normality and homogeneity of variance, as described above for evaluation of differences between groups of individual elastic system components.

We used stepwise comparison of Akaike information criterion (AIC) values (stepAIC R Mass package; Venables and Ripley, 2002) to determine the parameters and coefficients of the full model that best predicted elastic energy storage potential across natural variation of joint postures in preparation for jumps. The full statistical model evaluated included stored strain energy (PE) as a dependent factor and, as potential independent variables, tendon stiffness (tendonK), the summed maximum isometric force capacity of LG and MG along the tendon (sumFMax), the average LG and MG optimal fascicle length (avOFL) and starting muscle length at zero activation of the LG and MG in the pre-jump posture (avLenA0c). We included possible interaction terms between muscle force capacity, tendon stiffness and muscle start length (sumMaxF×tendonK×avLenA0c) and between optimal fascicle length and tendon stiffness (avOFL×tendonK) following recommendations by Zajac (1989) of functional equivalent muscle tendon joint properties. We did not include muscle moment arm or tendon slack length in the statistical model because they both contributed to the starting muscle length at any given joint posture.

To quantify the relative explanatory power of morphological variation of any individual element to predict stored energy to a systems-level approach, we compared individual parameter models with the best multi-parameter model found by stepwise comparisons described above. The AIC value of the best model was compared with AIC values of models with individual predictors and their relative explanatory power was computed (Wagenmakers and Farrell, 2004).

The relationship between Achilles tendon elastic energy storage capacity and experimentally measured muscle-mass-normalized peak power output and jump work were both tested with a linear model with elastic energy storage as the dependent variable and peak power or jump work as the independent variable.

RESULTS

Variation in individual elements of the elastic system

We found no statistically significant differences in any individual morphological property between birds that jumped during growth and those that did not (all $P \geq 0.1$; Tables 1, 2).

Energy storage capacity between groups

We found no significant differences in the capacity to store energy in the strain of elastic elements between birds restricted and unrestricted from high power activities during maturation, despite small differences in tendon strain that did not reach significance (Table 3, Fig. 3). This held true both at the peak crouched posture before jump initiation (P=0.43; Fig. 2C) and at the posture that optimized elastic energy storage (P=0.44; Fig. 2D). It should be noted that the optimum posture for elastic energy storage was at the most extended knee angle and the most flexed ankle angle tested, and was an ∼85 deg more extended ankle angle than birds used in preparation for a jump. While this more extended posture lengthened the gastrocnemius and increased the energy stored in the Achilles, it shortened the operating length of the knee extensor muscles, reducing their force-generating capacity. In the pre-jump posture, the shorter gastrocnemius length decreased elastic storage capacity by 12% for control birds and 10% for restricted birds (Table 3) in comparison to the optimal posture for energy storage.

Morphological predictors of elastic energy storage capacity

We found that the amount of energy stored in strain of the tendon was best explained by variation in the average of the passive LG and MG muscle length at activation onset, avLenA0 (Table 4). Fig. 4A illustrates that tendon strain energy increases at longer starting lengths both between individuals and, even more strikingly, within individuals, across postures. Muscle force capacity along the tendon was the next most explanatory variable and, like normalized muscle length, shows a positive relationship with energy storage (Fig. 4B). In contrast, longer muscle optimal fascicle lengths reduced energy storage (P=0.03; Table 4, Fig. 4D) when evaluated as an individual predictor, but was not a significant factor as a predictor in the full

Journal of Experimental Biology (2021) 224, jeb242694. doi:10.1242/jeb.242694

Table 3. Comparison of energy storage capacity and normalized fiber length between restricted and unrestricted birds at maturity at the posture that maximized tendon strain across all postures and in the pre-jump posture

	Restricted	Control	*P*
At max. strain energy posture			
Energy storage potential (J)	0.3±0.065	0.26±0.12	0.44
Tendon strain	0.12±0.016	0.098±0.021	0.031
Average normalized fiber length at A0	1.1±0.051	0.99±0.098	0.11
Average normalized fiber length at A100	0.75±0.051	0.72±0.054	0.27
Knee angle at max. PE (deg)	−131±1.9	−130±0	1
Ankle angle at max. PE (deg)	−45±0	−45±0	1
In pre-jump posture (knee: −135 deg; ankle: 120 deg)			
Energy storage potential (J)	0.27±0.055	0.23±0.11	0.43
Tendon strain	0.12±0.015	0.094±0.021	0.028
Average normalized fiber length at A0	1±0.05	0.96±0.097	0.11
Average normalized fiber length at A100	0.73±0.048	0.7±0.051	0.28

PE, stored strain energy. Normalized muscle length at the start and end of contraction designated by average normalized fiber length at A0 and A100, respectively.

multi-parameter model. Opposite to our predictions, tendon stiffness did not significantly correlate with elastic strain energy when evaluated as an individual predictor (P>0.1; Table 4, Fig. 4C), but did improve the explanatory power of a full model. The stepwise AIC comparison of full and reduced models found the sum of LG and MG maximum force capacity along the tendon (sumFMax), average optimal fascicle length (avOFL), muscle length at activation onset (avLenA0), tendon stiffness and the interaction of tendon stiffness and muscle force capacity as the independent predictors that best correlated with stored elastic strain energy. The relative explanatory power of each predictor followed similar patterns as seen in the individual analyses, with muscle start length and force capacity showing the greatest predictive power. This full model had an R^2 of 0.93 and was over 280,000 times more likely to explain the variation in strain energy than any model with only one explanatory variable.

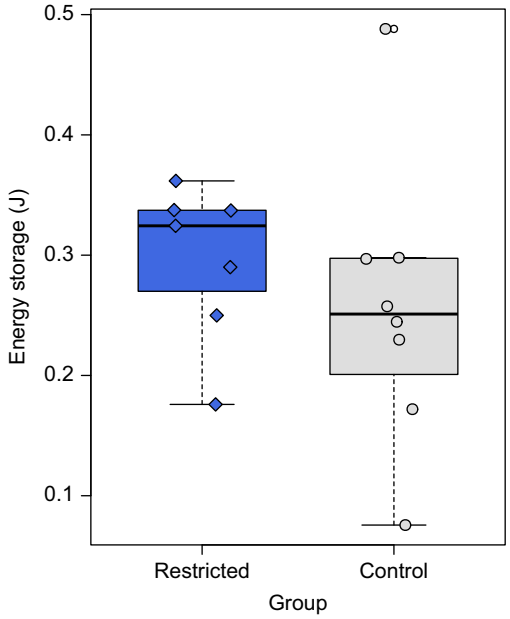

Fig. 3. Restricting high power activities in restricted birds (blue) does not decrease or significantly influence the capacity to store elastic strain energy compared with controls (grey). Each marker represents data from one individual guinea fowl.

Energy storage capacity versus jump performance

We found little to no correlation between energy storage capacity predicted by simulations and experimentally collected jump metrics of either muscle-mass-specific work or power (Fig. 5). A linear model showed no significant relationship between either peak power or jump power per kilogram of muscle mass capacity (t=−0.36, P=0.72, R^2_{adj}=−0.07) or jump work (t=−0.05, P=0.96, R^2_{adj}=−0.08) and strain energy in the pre-jump posture. The negative adjusted R^2 values for both tests show that the variation in jump work or peak power explains only a negligible amount of variation in elastic energy storage potential. The scatterplot of standardized predicted values versus standardized residuals for both variables showed that the data met the assumptions of homogeneity of variance and linearity and the residuals were approximately normally distributed.

DISCUSSION

We found the gastrocnemius elastic system of the guinea fowl robust to variations in locomotor conditions during growth. Neither properties of individual components nor energy storage capacity varied between birds that did and did not jump throughout maturation. Nor did we find any correlation between energy storage capacity and jump performance. Variation in muscle operating length across individuals predicted energy storage capacity better than any fixed morphological property, and a systems approach incorporating multiple components was substantially able to predict energy storage capacity better than variation along any individual element.

Do components of the gastrocnemius elastic system change systematically in response to changes in power and work demand during growth?

Contrary to our predictions, we saw, in general, no systematic changes in the gastrocnemius elastic system in response to decreased demand for high power and work activities during maturation. Surprisingly, birds that were restricted from jumping throughout their entire growth period (Table 1) developed elastic systems that were largely indistinguishable from the control group that jumped, on average, almost 200 times a day.

Two factors may account for why we saw no systematic changes in the elastic system whereas observations of morphological plasticity in response to changes in functional demand abound (Baldwin and Haddad, 2002; Blazevich et al., 2003; Fitts and Widrick, 1996; Mcdonagh and Davies, 1984; Wisdom et al., 2015), even in guinea fowl in particular (Buchanan and Marsh, 2001; Salzano et al., 2018). First, several studies suggest that plasticity may vary by life stage, with lower or inconsistent plasticity in growing animals (Aucouturier et al., 2008; Johnston, 2006; Legerlotz et al., 2016). Thus, the inconsistency between the lack of plasticity in our study and the morphological variation found by others suggests that guinea fowl may exhibit lower plasticity during maturation than in adulthood. Fast-growing species, such as guinea fowl, might outpace environmental fluctuations with rapid growth and not invest in developmental plasticity (Dewitt et al., 1998; Snell-Rood, 2012). A slow-growing species (humans, for example) might have a selective advantage with greater developmental plasticity. Thus, although our treatment may have been powerful

Journal of Experimental Biology (2021) 224, jeb242694. doi:10.1242/jeb.242694

Table 4. Results of models comparing how well variation of individual elastic elements explain variation in elastic storage potential (shaded regions) and stepwise model comparisons of models with multiple predictors (unshaded region)

	Coeff.	Adj. R^2	*P*	AIC	ΔAIC (1–5)	w(AIC)	*L*(null|*x*)	ΔAIC (2–6)	w(AIC)	*L*(full|*x*)
1. Null				–28	0	1.1e–5	1			
2. sumFMax	0.002	0.50	2.0e–3	–37	–9.4	1.2e–3	111	28	1.6e21	1.0e6
3. tendonK	–1.3e–8	–0.077	1	–26	2.0	3.1e–6	0.37	39	5.3e18	3.0e8
4. avLenA0	0.40	0.57	6.4e–4	–40	–12	3.3e–3	390	25	5.6e21	2.8e5
5. avOFL	–1.5	0.26	3.1e–2	–31	–3.6	5.1e–5	6	33	8.6e19	1.9e7
6. Full:		0.93	2.3e–6	–65				0	1.5e27	1
sumFMax	6.1e–3		3.2e–4							
tendonK	1.2e–5		0.02							
avLenA0	0.29		2.0e–4							
avOFL	0.78		0.07							
sumFMax×tendonK	–7.1e–8		4.5e–3							

Muscle operating length at the start of activation (avLenA0) is most predictive of energy storage, with muscle force capacity, the sum of lateral and medial maximum isometric force (sumFMax), and average gastrocnemius optimal fiber length (avOFL) also significant. Tendon stiffness (tendonK) added little to no additional predictive information. A multi-predictor model (Full: darker shaded region) explained variation in energy storage capacity over 160,000 times better than any individual predictor. Likelihood comparisons between the null and individual models are designated by L(null|*x*), and between the full model and individual predictor models by L(full|*x*). Akaike weights are listed under w(AIC).

enough to induce morphological changes in adults, rapidly growing guinea fowl may be more robust to environmental perturbations.

Second, our results could be consistent with the results of other studies if the plastic response to decreased demand is not inferable from changes in response to increases in demand. For example, it may be that the increase in muscle mass that occurs in response to a certain increase in functional demand is greater than the decrease in muscle mass that occurs in response to the equivalent decrease in demand.

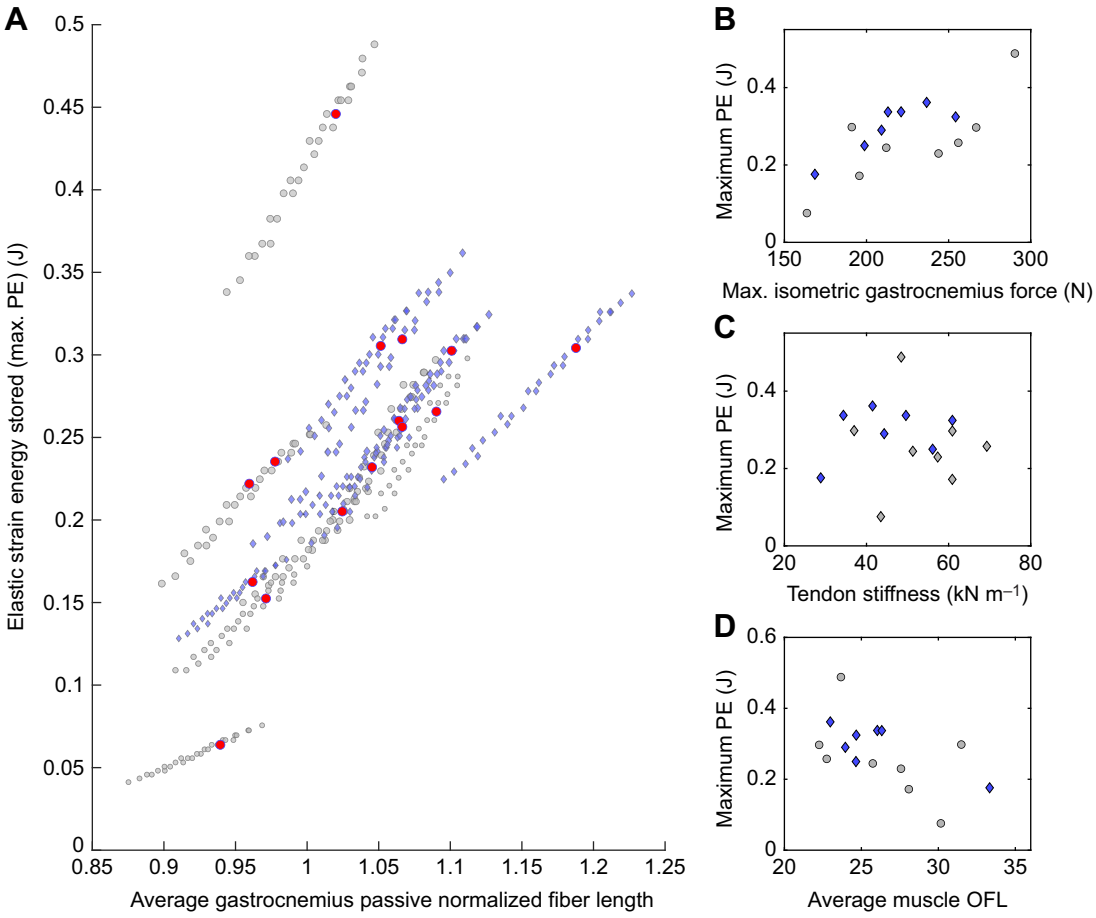

Fig. 4. Correlations between morphological variation of individual components of the gastronomicnemius elastic system and stored elastic potential energy. Energy stored in the tendon increases with passive normalized fiber length (length at onset of muscle activation) across different postures (A) and muscle force capacity (B), decreases with muscle optimal fiber length (D), but did not consistently vary with tendon stiffness (C). The variable that most predicts elastic strain energy is muscle normalized fiber length at activation onset (A), with muscles operating at longer lengths enabling greater elastic energy storage. Color and shape designate group (blue diamond, restricted; grey circle, control). In A, red dots identify the strain energy stored and normalized fiber length in the pre-jump posture. In B, C and D, each marker represents data from one individual guinea fowl. See Table 4 for corresponding statistical results.

Journal of Experimental Biology (2021) 224, jeb242694. doi:10.1242/jeb.242694

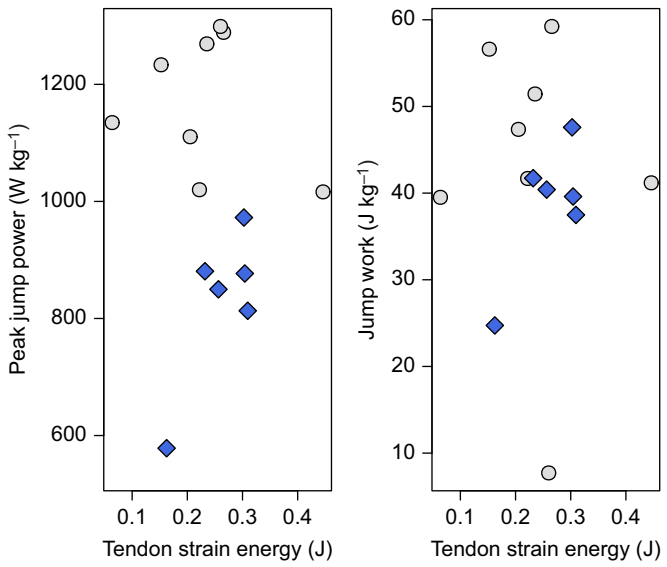

Fig. 5. Neither peak jump power nor jump work increase systematically with maximum tendon strain energy across all individuals. Markers designate data from one individual guinea fowl in pre-jump posture, and color and marker differentiate treatment groups (grey circle, control; blue diamond, restricted).

Many studies find clear evidence of morphological plasticity, but this was in response to increased mechanical load (Atherton and Smith, 2012; Buchanan and Marsh, 2001; Kubo et al., 2007; Mcdonagh and Davies, 1984; Mersmann et al., 2017; Salzano et al., 2018) and extreme disuse (Bajotto and Shimomura, 2007; Campbell et al., 2013; Clark, 2009). Our intervention, however, eliminated jumping while maintaining consistent low intensity exercise (i.e. walking). Thus, we did not induce chronic offloading, as had been the goal in several previous disuse studies. Our results suggest that there may not be a linear dose–response relationship between changes in functional demand and morphological variation. Instead, as recently suggested (Katugam et al., 2020), there may be a range of variation in demand that is not extreme enough to induce physiological or morphological modifications above those under developmental control. If this region of stasis encompasses a wider range of disuse, it could explain both why offloading studies often require extreme disuse, such as bedrest or limb immobilization (Bajotto and Shimomura, 2007; Bebout et al., 1993; Clark, 2009), to induce change, and why we found no systematic morphological changes here. Eliminating jumping may not be an extreme enough disuse signal to induce musculoskeletal plasticity.

Thus, although we found no systematic morphological variation when restricting high power activities during maturation, this does not necessarily imply that the morphology of elastic systems does not plastically adapt to variations in functional demand. But it does suggest that there are conditions in which elastic systems may be insensitive to functional variation.

Is the energy storage capacity reduced in individuals that did not jump during growth?

Despite this lack of consistent morphological variation between our treatment groups, restricted birds showed performance deficits. This suggests either that small morphological changes in individual elastic elements compound to alter elastic system function, that variations are significant in other MTUs that we did not quantify, or that behavioral or neural variation account for the difference in jumping performance. Our systems-level analysis aimed to specifically address the question of whether morphological variation compound within the elastic system to enable unrestricted birds to store more energy in their Achilles tendon in preparation for a jump. Again, contrary to our predictions, simulations in our subject-specific models resulted in no differences between groups in their maximum ability to store elastic energy. Taken together, the findings of minimal changes to individual MTU components and no effect on the overall elastic energy storage could indicate that morphology necessary to enable jumping is highly conserved. This could happen if rapid movements are very critical to fitness, as may be the case for prey animals for whom evasion is critical.

Which type of morphological variation has the greatest influence on energy storage capacity?

The first two analyses focus on plasticity of elastic systems and quantified the influence of rearing conditions on the morphology of individual components and how that variation influenced energy storage capacity across treatment groups. Our last two analyses utilize the variation within and across our treatment groups to further probe the relationship between form and function in elastic systems.

Evaluating the best predictors of energy storage, we found that muscle properties far outweighed the influence of tendon stiffness. Surprisingly, maximum isometric muscle force, while correlating with energy storage, was not the most important factor. Instead, normalized muscle length at the start of contraction was the best individual predictor of energy storage, with the longest normalized muscle lengths enabling greatest elastic storage [in agreement with results from Azizi and Roberts (2010) and Rosario et al. (2016)]. This may be because muscles that start contracting on the descending or plateau region of the force–length curve increase force capacity as they shorten, resulting in a greater equilibrium force, while muscles starting on the ascending limb of the force–length curve lose force capacity as they shorten against a tendon during an isometric contraction (Cox et al., 2019b). Further, we were particularly surprised to find that tendon stiffness alone had little to no predictive power of energy storage. Together, these data suggest that, between individuals or across an individual's lifetime, the large variation in force capacity owing to force–length or force–velocity effects may overshadow the influence of variation in tendon properties in determining tendon strain energy. This conclusion is consistent with studies in humans that found no correlation between tendon stiffness and vertical jump height (Kubo et al., 1999). Yet, this idea runs contrary to the focus on spring properties (Albracht and Arampatzis, 2006; Biewener and Roberts, 2000; Bohm et al., 2019; Fletcher and MacIntosh, 2018; Khayyeri et al., 2017; Proske and Morgan, 1987; Waugh et al., 2012, 2014) or relative spring and maximal muscle properties (Lichtwark and Wilson, 2008; Mersmann et al., 2017) in many studies that try to connect form and function in elastic systems. Our results suggest that instead, between or within individuals, elastic energy storage capacity may be more sensitive to variations that alter muscle operating lengths (tendon slack length, optimal fascicle lengths, joint postures) or muscle cross-sectional area than to changes in the tendons themselves.

Further, our results also highlight the importance of analyzing the components of an elastic system in concert rather than trying to infer performance from variation in one component. Our full model that included both muscle (maximum muscle force and starting length) and tendon properties explained changes in energy storage capacity over 280,000 times better than variation in any individual property, even when penalizing models for complexity. This, again, emphasizes the limitations of reductionist approaches

Journal of Experimental Biology (2021) 224, jeb242694. doi:10.1242/jeb.242694

to understanding how musculoskeletal morphological variation influences the energy storage capacity of an elastic system.

Does elastic energy storage capacity predict peak jump powers and work?

Contrary to our expectations, individuals that developed elastic systems capable of storing greater energy in their tendons did not take advantage of that ability to produce more powerful jumps. This suggests that morphology may play a smaller role than neural control in determining contribution of elastic energy storage in jumping. Musculoskeletal morphological variation may not be the main factor limiting jump performance.

The interaction between tendon and muscle force–length curves may, in part, provide a mechanistic explanation for this disconnect between morphology and performance. Here, we include a conceptual diagram to illustrate how variations in morphology (here maximum muscle force capacity) may be less influential than properties that can be adjusted in real time (here muscle start length) (Fig. 6). If we plot the muscle and tendon force–length curves on the same figure, it is possible to visualize how they might interact. If the muscle operates on the ascending or plateau region of the force length curve, where passive forces are minimal, and we assume that there is no slack in the tendon, a tendon strain of zero will coincide with the muscle length at the start of a contraction. Any tendon length change, then, is equal and opposite to the change in muscle length. During a fixed-end contraction, the maximal tendon strain occurs when the tendon force equals the total muscle force of the three heads of the gastrocnemius (open circles, Fig. 6). The tendon strain at equilibrium, then, is dramatically influenced by the length of the muscle when it begins to contract (Fig. 6A), reaching higher values for contractions starting at longer muscle lengths. As our results suggest (and as can be visualized by comparing the differences in the areas of the grey shaded regions between Fig. 6A and B), these dynamics can be larger than the influence of naturally occurring variations in maximal force capacity. Although we constrained this thought experiment to muscles operating on the ascending or plateau region of the force–length curve because those were the operating lengths that correspond to the range of joint angles observed in this species and are most common in vertebrates (Burkholder et al., 2001), it is interesting to note that the above argument may not hold true for muscles starting at longer lengths. Although starting at longer lengths further increases energy storage for a given muscle (both muscle force capacity and tendon resistance increasing with muscle shortening), increasing force capacity for muscles starting on the descending limb also drastically increases energy storage capacity. Thus, although changes in operating lengths many not always be more influential on energy storage than changes in force capacity, muscle start length can dramatically alter energy storage potential of an elastic system in all conditions. And although muscle operating lengths are constrained by morphology (OFL, pennation angle and moment arms), they are also easily varied with joint angle. Large variations in maximum muscle force could be compensated for by small variations in posture largely under neural control. Thus, as our results suggest, dynamic factors such as muscle operating length may influence energy storage more than temporarily fixed musculoskeletal features such as maximum muscle force capacity.

This suggests that there may be a large range of morphological variation that can be compensated for with neural plasticity and brings up questions of how the two interact. Does variation along a particular morphological axis correlate with systematic changes in neural control? If so, how do individuals search though the neural possibility space? What are the limits of neural compensation? Do we see greater morphological plasticity of the components of elastic systems in conditions that push the limits of neural plasticity?

Potential interactions between musculoskeletal and neural variation in elastic energy storage

Although musculoskeletal morphology may set the bounds of possible energy storage, individuals may not operate at their limits of elastic potential. This suggests either a significant behavioral component (restricted birds simply may have not tried as hard to jump) or that there may be benefits to real-time tunability in elastic systems. The jump of a guinea fowl is powered by both tendon recoil and simultaneous muscle work (Henry et al., 2005), as is common in many larger animals (Alexander, 1974, 1995; Kubo et al., 1999; Roberts and Marsh, 2003). The muscles that load the tendon pre-jump also contract during take-off to contribute power to the jump. In these hybrid systems, trade-offs between maximizing tendon strain energy and muscle power may explain our finding that the pre-jump posture of guinea fowl did not optimize energy storage in the tendon. Adjusting muscle lengths to maximize tendon strain may hamper muscle fiber work during take-off. Further, in a complex system such as this, with dozens of individual MTUs spanning multiple joints and working in concert with direct drive muscles with little tendon, the difference between a great jumper and a good jumper might depend less on the maximal storage capacity of any one MTU (i.e. its musculoskeletal morphology) and more on fine

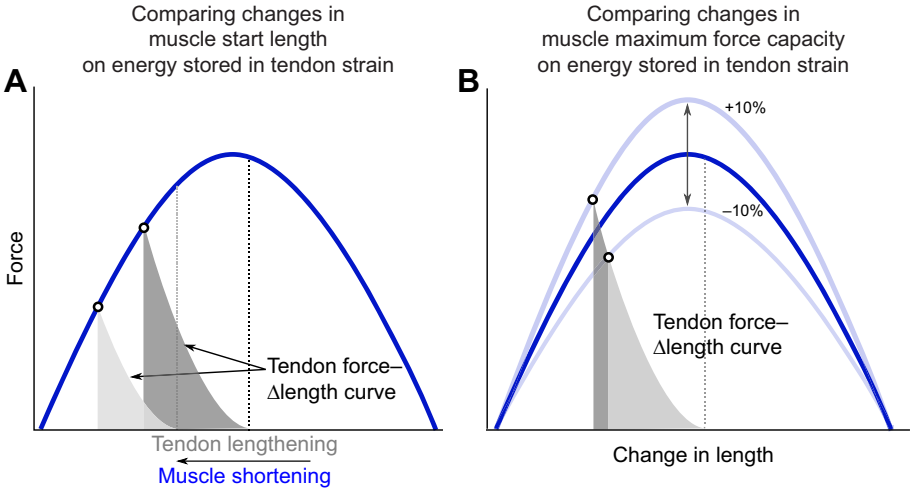

Fig. 6. The energy stored in the tendon during a fixed-end contraction is constrained by the interaction of the muscle (blue curve) and tendon force–Δ length curves (grey curve). As tendon length changes must be equal and opposite to muscle length changes, we can plot them at the same scale. Changes in muscle length at the onset of contraction (A) can have a larger influence on energy storage than variations in muscle force capacity (B). The variation in maximum muscle force depicted here represent variation observe in our subjects. Here, changes in start length (0.9–1.2) and muscle force capacity (±10%) reflect experimentally measured variation in our population.

adjustments of neural control to harmonize the output of the collective system (Adkins et al., 2006; Enoka, 1997; Häkkinen et al., 2000).

Together, our experimental and modeling analyses suggest that performance advantage of the control birds, which practiced jumping throughout maturation, may lie less in the body's modification of individual elastic elements, and more in the fine tuning of neural circuits to coordinate muscle activation timing to take better advantage of what they each possess. Although restricting normal locomotor behavior during growth (i.e. eliminating practice) likely leads to deficits in neural control, neural plasticity is potentially a rapidly reversible pathway to adapt an elastic system to functional variation. Given the potential short timescale of neural plasticity (Adkins et al., 2006; Yoxon and Welsh, 2019), greater sensitivity of neural locomotor/movement stimuli could allow the individual to adjust the dynamics of an elastic system during growth without making potentially irreversible changes to morphology that could be detrimental in subsequent stages of growth or in adulthood if environmental conditions or functional demand rapidly change. Thus, one could interpret the results of our study as suggesting that practice during growth may indeed be more related to forming the neural framework for jumping than for forming the musculoskeletal framework. This also suggests the specific hypothesis that individuals restricted from an activity during growth may be capable of reversing the resulting neural deficits with practice later in life.

Limitations

Several modeling simplifications could have influenced our results. For instance, the gastrocnemius elastic system is not the only one that could contribute to jump power. Although the Achilles is the largest tendon involved, many other digital tendons spanning both the ankle and tarsometatarsus joint have the potential to contribute to jump power but were not included in our analysis. Furthermore, changes in the characteristics of muscles spanning proximal joints may also have contributed to the differences in jump power, but these muscles were not modeled. Additionally, potentially important dynamic effects were ignored. For simplicity, we simulated the amount of energy stored in the Achilles tendon during fixed-end contractions, where the joint posture was constant as the muscle and tendon dynamically responded to increasing muscle activation. Activating muscles while altering joint posture would alter these dynamics, perhaps amplifying the influence of individual differences in input or output lever lengths or force–velocity effects not apparent from group averages. Likewise, we did not measure potential variation in muscle-specific tension, which could alter our estimates of maximal muscle force capacity. Nor did we measure and include individual variation in muscle or aponeurosis passive elastic properties that could significantly alter energy storage (Arellano et al., 2019; Huijing and Ettema, 1988; Lemos et al., 2008). Although this is a common approach in musculoskeletal modeling (Millard et al., 2013; Seth et al., 2018; Zajac, 1989), variation in the aponeurosis and free tendon stiffness (Ettema and Huijing, 1989; Finni, 2006) have the potential to introduce errors (Epstein et al., 2006; Lieber et al., 2017).

Another possible limitation was the modeling choice to focus on the potential for an individual to store energy in the strain of their tendon. How that energy is released and how that energy release interacts with synchronous muscle activation could also influence jump performance (Ilton et al., 2018). Because jumps are likely powered both by tendon recoil and muscle work (Azizi and Roberts, 2010; Henry et al., 2005), there may be a trade-off between the work the muscle puts into tendon strain and that which is left available to power the jump during tendon recoil (Sutton et al., 2019). Future work could involve simulation of jumps in these subject-specific models to assess the contributions of these dynamic factors. Thus, although we found no consistent change in components of the gastrocnemius elastic system owing to decreased demand for high power activities during growth, more complex models may provide insight into the ways in which morphological variation constrains performance.

Conclusions

We found that decreasing the demand for high power and work during growth can influence adult performance but does not necessarily lead to morphological plasticity. We found no difference in energy storage capacity between groups that did and did not jump throughout maturation or any correlation with experimentally measured jump performance. We conclude that the gastrocnemius elastic system in the guinea fowl displays little to no morphological plastic response to decreased demand during growth and that neural control of elastic systems may constrain performance more than morphology.

Acknowledgements

We thank Dr Kirsty McDonald and Justin Csaszar for help collecting this data. We also thank the staff at the Central Biological Laboratory at The Pennsylvania State University for their care of our animals during the study and Dennis Ripka for support building housing.

Competing interests

The authors declare no competing or financial interests.

Author contributions

Conceptualization: S.M.C., S.J.P., J.R.; Methodology: S.M.C.; Software: S.M.C.; Validation: S.M.C.; Formal analysis: S.M.C., M.Q.S.; Investigation: S.M.C., A.D., M.Q.S., K.K.; Resources: J.R.; Data curation: S.M.C.; Writing - original draft: S.M.C.; Writing - review & editing: S.M.C., A.D., M.Q.S., K.K., S.J.P., J.R.; Visualization: S.M.C.; Supervision: J.R.; Project administration: J.R.; Funding acquisition: S.J.P., J.R.

Funding

This study was supported in part through a seed grant from the Center for Human Evolution and Diversity, The Pennsylvania State University, and through the National Institute of Arthritis and Musculoskeletal and Skin Diseases of the National Institutes of Health under grant number R21AR071588. The content is solely the responsibility of the authors of this paper and does not necessarily represent the views of the National Institutes of Health. Deposited in PMC for release after 12 months.

Data availability

Data are available from the Dryad digital repository (Cox et al., 2021): doi:10.5061/dryad.w3r2280r7.

References

Ackland, D. C., Lin, Y.-C. and Pandy, M. G. (2012). Sensitivity of model predictions of muscle function to changes in moment arms and muscle-tendon properties: a Monte-Carlo analysis. *J. Biomech.* **45**, 1463-1471. doi:10.1016/j.jbiomech.2012.02.023

Adkins, D. L., Boychuk, J., Remple, M. S. and Kleim, J. A. (2006). Motor training induces experience-specific patterns of plasticity across motor cortex and spinal cord. *J. Appl. Physiol.* **101**, 1776-1782. doi:10.1152/japplphysiol.00515.2006

Ahn, A. N., Monti, R. J. and Biewener, A. A. (2003). In vivo and in vitro heterogeneity of segment length changes in the semimembranosus muscle of the toad. *J. Physiol.* **549**, 877-888. doi:10.1113/jphysiol.2002.038018

Albracht, K. and Arampatzis, A. (2006). Influence of the mechanical properties of the muscle-tendon unit on force generation in runners with different running economy. *Biol. Cybern.* **95**, 87-96. doi:10.1007/s00422-006-0070-z

Alexander, R. (1968). *Animal Mechanics*. University of Washington Press.

Alexander, R. M. (1974). The mechanics of jumping by a dog. *J. Zool.* **173**, 549-573. doi:10.1111/j.1469-7998.1974.tb04134.x

Alexander, R. M. (1995). Leg design and jumping technique for humans, other vertebrates and insects. *Philos. Trans. R. Soc. Lond. B. Biol. Sci.* **347**, 235-248. doi:10.1098/rstb.1995.0024

Arellano, C. J., Konow, N., Gidmark, N. J. and Roberts, T. J. (2019). Evidence of a tunable biological spring: Elastic energy storage in aponeuroses varies with transverse strain in vivo. *Proc. R. Soc. B Biol. Sci.* **286**, 3-8. doi:10.1098/rspb.2018.2764

Astley, H. C. and Roberts, T. J. (2012). Evidence for a vertebrate catapult: elastic energy storage in the plantaris tendon during frog jumping. *Biol. Lett.* **8**, 386-389. doi:10.1098/rsbl.2011.0982

Astley, H. C. and Roberts, T. J. (2014). The mechanics of elastic loading and recoil in anuran jumping. *J. Exp. Biol.* **217**, 4372-4378. doi:10.1242/jeb.110296

Atherton, P. J. and Smith, K. (2012). Muscle protein synthesis in response to nutrition and exercise. *J. Physiol.* **590**, 1049-1057. doi:10.1113/jphysiol.2011.225003

Aucouturier, J., Baker, J. S. and Duché, P. (2008). Fat and carbohydrate metabolism during submaximal exercise in children. *Sport. Med.* **38**, 213-238. doi:10.2165/00007256-200838030-00003

Azizi, E. and Deslauriers, A. R. (2014). Regional heterogeneity in muscle fiber strain: the role of fiber architecture. *Front. Physiol.* **5**, 303. doi:10.3389/fphys.2014.00303

Azizi, E. and Roberts, T. J. (2010). Muscle performance during frog jumping: influence of elasticity on muscle operating lengths. *Proc. A R. Soc. B* **277**, 1523-1530. doi:10.1098/rspb.2009.2051

Bajotto, G. and Shimomura, Y. (2007). Determinants of disuse-induced skeletal muscle atrophy: exercise and nutrition countermeasures to prevent protein loss. *J. Nutr. Sci. Vitaminol.* **52**, 233-247. doi:10.3177/jnsv.52.233

Baldwin, K. M. and Haddad, F. (2002). Skeletal muscle plasticity: Cellular and molecular responses to altered physical activity paradigms. *Am. J. Phys. Med. Rehabil.* **81**, 40-51. doi:10.1097/00002060-200211001-00006

Bebout, D. E., Hogan, M. C., Hempleman, S. C. and Wagner, P. D. (1993). Effects of training and immobilization on VO2 and DO2 in dog gastrocnemius muscle in situ. *J. Appl. Physiol.* **74**, 1697-1703. doi:10.1152/jappl.1993.74.4.1697

Biewener, A. and Baudinette, R. (1995). *In vivo* muscle force and elastic energy storage during steady-speed hopping of tammar wallabies (*Macropus eugenii*). *J. Exp. Biol.* **198**, 1829-1841. doi:10.1242/jeb.198.9.1829

Biewener, A. A. and Roberts, T. J. (2000). Muscle and tendon contributions to force, work, and elastic energy savings: a comparative perspective. *Exercise Sport Sci. Rev.* **28**, 99-107.

Biewener, A. A., McGowan, C., Card, G. M. and Baudinette, R. V. (2004). Dynamics of leg muscle function in tammar wallabies (*M. eugenii*) during level versus incline hopping. *J. Exp. Biol.* **207**, 211-223. doi:10.1242/jeb.00764

Blazevich, A. J., Gill, N. D., Bronks, R. and Newton, R. U. (2003). Training-specific muscle architecture adaptation after 5-wk training in athletes. *Med. Sci. Sports Exerc.* **35**, 2013-2022. doi:10.1249/01.MSS.0000099092.83611.20

Bohm, S., Mersmann, F., Tettke, M., Kraft, M. and Arampatzis, A. (2014). Human Achilles tendon plasticity in response to cyclic strain: effect of rate and duration. *J. Exp. Biol.* **217**, 4010-4017. doi:10.1242/jeb.112268

Bohm, S., Mersmann, F. and Arampatzis, A. (2019). Functional adaptation of connective tissue by training. *Dtsch. Z. Sportmed.* **70**, 105-109. doi:10.5960/dzsm.2019.366

Buchanan, C. I. and Marsh, R. L. (2001). Effects of long-term exercise on the biomechanical properties of the Achilles tendon of guinea fowl. *J. Appl. Physiol.* **90**, 164-171. doi:10.1152/jappl.2001.90.1.164

Buchanan, T. S., Lloyd, D. G., Manal, K. and Besier, T. F. (2004). Neuromusculoskeletal modeling: estimation of muscle forces and joint moments and movements from measurements of neural command. *J. Appl. Biomech.* **20**, 367-395. doi:10.1123/jab.20.4.367

Burkholder, T. J., Lieber, R. L. and Burkholder, T. J. (2001). Sarcomere length operating range of vertebrate muscles during movement. *J. Exp. Biol.* **204**, 1529-1536. doi:10.1242/jeb.204.9.1529

Campbell, E. L., Seynnes, O. R., Bottinelli, R., McPhee, J. S., Atherton, P. J., Jones, D. A., Butler-Browne, G. and Narici, M. V. (2013). Skeletal muscle adaptations to physical inactivity and subsequent retraining in young men. *Biogerontology* **14**, 247-259. doi:10.1007/s10522-013-9427-6

Carr, J. A., Ellerby, D. J. and Marsh, R. L. (2011). Differential segmental strain during active lengthening in a large biarticular thigh muscle during running. *J. Exp. Biol.* **214**, 3386-3395. doi:10.1242/jeb.050252

Clark, B. C. (2009). In vivo alterations in skeletal muscle form and function after disuse atrophy. *Med. Sci. Sports Exerc.* **41**, 1869-1875. doi:10.1249/MSS.0b013e3181a645a6

Cox, S., Salzano, M., DeBoef, A., Piazza, S. and Rubenson, J. (2019a). *Decreased Physical Activity During Growth Reduces Peak force Capacity but not Running Economy in a Bipedal Animal Model*. Calgary: International Society of Biomechanics.

Cox, S. M., Easton, K. L., Lear, M. C., Marsh, R. L., Delp, S. L., Rubenson, J., Sanghvi, H., Cromie, M., Marsh, R. L., Delp, S. L. et al. (2019b). The interaction of compliance and activation on the force-length operating range and force generating capacity of skeletal muscle: a computational study using a guinea fowl musculoskeletal model. *Integr. Org. Biol.* **1**, 1-20.

Cox, S. M., Salzano, M. Q., Piazza, S. J. and Rubenson, J. (2020). Eliminating high-intensity activity during growth reduces mechanical power capacity but not submaximal metabolic cost in a bipedal animal model. *J. Appl. Physiol.* **128**, 50-58. doi:10.1152/japplphysiol.00679.2019

Cox, S., Rubenson, J., Piazza, S., Salzano, M., Katugam, K. and DeBoef, A. (2021). Plasticity of the gastrocnemius elastic system in response to decreased work and power demand during growth. *Dryad, Dataset*, doi:10.5061/dryad.w3r2280r7

De Groote, F., Van Campen, A., Jonkers, I. and De Schutter, J. (2010). Sensitivity of dynamic simulations of gait and dynamometer experiments to Hill muscle model parameters of knee flexors and extensors. *J. Biomech.* **43**, 1876-1883. doi:10.1016/j.jbiomech.2010.03.022

Dewitt, T. J., Sih, A. and Wilson, D. S. (1998). Costs and limits of phenotypic plasticity. *Trends Ecol. Evol.* **13**, 77-81. doi:10.1016/S0169-5347(97)01274-3

Docking, S. I. and Cook, J. (2019). How do tendons adapt? Going beyond tissue responses to understand positive adaptation and pathology development: a narrative review. *J. Musculoskelet. Neuronal Interact.* **19**, 300-310.

Du, T. Y. and Standen, E. M. (2017). Phenotypic plasticity of muscle fiber type in the pectoral fins of *Polypterus senegalus* reared in a terrestrial environment. *J. Exp. Biol.* **220**, 3406-3410. doi:10.1242/jeb.162909

Eliasson, P., Fahlgren, A., Pasternak, B. and Aspenberg, P. (2007). Unloaded rat Achilles tendons continue to grow, but lose viscoelasticity. *J. Appl. Physiol.* **103**, 459-463. doi:10.1152/japplphysiol.01333.2006

Enoka, R. M. (1997). Neural adapations with chronic physical activity. *J. Biomech.* **30**, 465-475. doi:10.1016/S0021-9290(96)00170-4

Epstein, M., Wong, M. and Herzog, W. (2006). Should tendon and aponeurosis be considered in series? *J. Biomech.* **39**, 2020-2025. doi:10.1016/j.jbiomech.2005.06.011

Estes, R. R., Malinowski, A., Piacentini, M., Thrush, D., Salley, E., Losey, C. and Hayes, E. (2017). The effect of high intensity interval run training on cross-sectional area of the vastus lateralis in untrained college students. *Int. J. Exerc. Sci.* **10**, 137-145.

Ettema, G. J. C. (1996). Elastic and length-force characteristics of the gastrocnemius of the hopping mouse (*Notomys alexis*) and the rat (*Rattus norvegicus*). *J. Exp. Biol.* **199**, 1277-1285. doi:10.1242/jeb.199.6.1277

Ettema, G. J. C. and Huijing, P. A. (1989). Properties of the tendinous structures and series elastic component of EDL muscle-tendon complex of the rat. *J. Biomech.* **22**, 1209-1215. doi:10.1016/0021-9290(89)90223-6

Farris, D. J., Lichtwark, G. A. J., Brown, N. A. T. and Cresswell, A. G. (2016). The role of human ankle plantar flexor muscle-tendon interaction and architecture in maximal vertical jumping examined in vivo. *J. Exp. Biol.* **219**, 528-534. doi:10.1242/jeb.126854

Finni, T. (2006). Structural and functional features of human muscle-tendon unit. *Scand. J. Med. Sci. Sport.* **16**, 147-158. doi:10.1111/j.1600-0838.2005.00494.x

Fitts, R. H. and Widrick, J. J. (1996). Muscle mechanics: adapations with exercise-training. *Exerc. Sport Sci. Rev.* **24**, 427-474. doi:10.1249/00003677-199600240-00016

Fletcher, J. R. and MacIntosh, B. R. (2018). Changes in Achilles tendon stiffness and energy cost following a prolonged run in trained distance runners. *PLoS ONE* **13**, e0202026. doi:10.1371/journal.pone.0202026

Galantis, A. and Woledge, R. C. (2003). The theoretical limits to the power output of a muscle–tendon complex with inertial and gravitational loads. *Proc. R. Soc. B Biol. Sci.* **270**, 1493-1498. doi:10.1098/rspb.2003.2403

Gillis, G. B. and Biewener, A. A. (2001). Hindlimb muscle function in relation to speed and gait: in vivo patterns of strain and activation in a hip and knee extensor of the rat (*Rattus norvegicus*). *J. Exp. Biol.* **204**, 2717-2731. doi:10.1242/jeb.204.15.2717

Häkkinen, K., Alen, M., Kallinen, M., Newton, R. U. and Kraemer, W. J. (2000). Neuromuscular adaptation during prolonged strength training, detraining and re-strength-training in middle-aged and elderly people. *Eur. J. Appl. Physiol.* **83**, 51-62. doi:10.1007/s004210000248

Henry, H. T., Ellerby, D. J. and Marsh, R. L. (2005). Performance of guinea fowl *Numida meleagris* during jumping requires storage and release of elastic energy. *J. Exp. Biol.* **208**, 3293-3302. doi:10.1242/jeb.01764

Huijing, P. A. and Ettema, G. J. (1988). Length-force characteristics of aponeurosis in passive muscle and during isometric and slow dynamic contractions of rat gastrocnemius muscle. *Acta Morphol. Neerl. Scand.* **26**, 51-62.

Ilton, M., Saad Bhamla, M., Ma, X., Cox, S. M., Fitchett, L. L., Kim, Y., Koh, J.-S., Krishnamurthy, D., Kuo, C.-Y., Temel, F. Z. et al. (2018). The principles of cascading power limits in small, fast biological and engineered systems. *Science (80-)* **360**, eaao1082. doi:10.1126/science.aao1082

Johnston, I. A. (2006). Environment and plasticity of myogenesis in teleost fish. *J. Exp. Biol.* **209**, 2249-2264. doi:10.1242/jeb.02153

Kao, P.-C., Lewis, C. L. and Ferris, D. P. (2010). Short-term locomotor adaptation to a robotic ankle exoskeleton does not alter soleus Hoffmann reflex amplitude. *J. Neuroeng. Rehabil.* **7**, 33. doi:10.1186/1743-0003-7-33

Katugam, K., Cox, S. M., Salzano, M. Q., De Boef, A., Hast, M. W., Neuberger, T., Ryan, T. M., Piazza, S. J. and Rubenson, J. (2020). Altering the mechanical load environment during growth does not affect adult Achilles tendon properties in an avian bipedal model. *Front. Bioeng. Biotechnol.* **8**, 994. doi:10.3389/fbioe.2020.00994

Khayyeri, H., Blomgran, P., Hammerman, M., Turunen, M. J., Löwgren, A., Guizar-Sicairos, M., Aspenberg, P. and Isaksson, H. (2017). Achilles tendon compositional and structural properties are altered after unloading by botox. *Sci. Rep.* **7**, 13067. doi:10.1038/s41598-017-13107-7

Kubo, K., Kawakami, Y. and Fukunaga, T. (1999). Influence of elastic properties of tendon structures on jump performance in humans. *J. Appl. Physiol.* **87**, 2090-2096. doi:10.1152/jappl.1999.87.6.2090

Kubo, K., Morimoto, M., Komuro, T., Yata, H., Tsunoda, N., Kanehisa, H. and Fukunaga, T. (2007). Effects of plyometric and weight training on muscle–tendon complex and jump performance. *Med. Sci. Sport. Exerc.* **39**, 1801-1810. doi:10.1249/mss.0b013e31813e630a

Landsmeer, J. M. (1961). Studies in the anatomy of articulation. 1. The equilibrium of the "intercalated" bone. *Acta Morphol. Neerl. Scand.* **3**, 287-303.

Legerlotz, K., Marzilger, R., Bohm, S. and Arampatzis, A. (2016). Physiological adaptations following resistance training in youth athletes—a narrative review. *Pediatr. Exerc. Sci.* **28**, 501-520. doi:10.1123/pes.2016-0023

Lemos, R. R., Epstein, M. and Herzog, W. (2008). Modeling of skeletal muscle: The influence of tendon and aponeuroses compliance on the force-length relationship. *Med. Biol. Eng. Comput.* **46**, 23-32. doi:10.1007/s11517-007-0259-x

Lewis, G. S., Sommer, H. J. and Piazza, S. J. (2006). *In vitro* assessment of a motion-based optimization method for locating the talocrural and subtalar joint axes. *J. Biomech. Eng.* **128**, 596-603. doi:10.1115/1.2205866

Lichtwark, G. A. and Wilson, A. M. (2008). Optimal muscle fascicle length and tendon stiffness for maximising gastrocnemius efficiency during human walking and running. *J. Theor. Biol.* **252**, 662-673. doi:10.1016/j.jtbi.2008.01.018

Lieber, R. L., Roberts, T. J., Blemker, S. S., Lee, S. S. M. and Herzog, W. (2017). Skeletal muscle mechanics, energetics and plasticity. *J. Neuroeng. Rehabil.* **14**, 108. doi:10.1186/s12984-017-0318-y

Lutz, G. J. and Rome, L. C. (1996). Muscle function during jumping in frogs. I. Sarcomere length change, EMG pattern, and jumping performance. *Am. J. Physiol.* **271**, C563-C570. doi:10.1152/ajpcell.1996.271.2.C563

Mayfield, D. L., Launikonis, B. S., Cresswell, A. G. and Lichtwark, G. A. (2016). Additional in-series compliance reduces muscle force summation and alters the time course of force relaxation during fixed-end contractions. *J. Exp. Biol.* **219**, jeb143123. doi:10.1242/jeb.143123

Mcdonagh, M. J. N. and Davies, C. T. M. (1984). Adaptive response of mammalian skeletal muscle to exercise with high loads. *Eur. J. Appl. Physiol.* **52**, 139-155. doi:10.1007/BF00433384

Mendez, J. and Keys, A. (1960). Density and composition of mammalian muscle. *Metabolism* **9**, 184-188. References - Scientific Research Publishing.

Mersmann, F., Charcharis, G., Bohm, S. and Arampatzis, A. (2017). Muscle and tendon adaptation in adolescence: Elite volleyball athletes compared to untrained boys and girls. *Front. Physiol.* **8**, 1-11. doi:10.3389/fphys.2017.00417

Millard, M., Uchida, T., Seth, A. and Delp, S. L. (2013). Flexing computational muscle: modeling and simulation of musculotendon dynamics. *J. Biomech. Eng.* **135**, 021005. doi:10.1115/1.4023390

Minamoto, V. B., Suzuki, K. P., Bremner, S. N., Lieber, R. L. and Ward, S. R. (2015). Dramatic changes in muscle contractile and structural properties after two Botulinum toxin injections. *Muscle Nerve* **52**, 649-657. doi:10.1002/mus.24576

Nishikawa, K., Biewener, A. A., Aerts, P., Ahn, A. N., Chiel, H. J., Daley, M. A., Daniel, T. L., Full, R. J., Hale, M. E., Hedrick, T. L. et al. (2007). Neuromechanics: an integrative approach for understanding motor control. *Integr. Comp. Biol.* **47**, 16-54. doi:10.1093/icb/icm024

Patek, S. N., Dudek, D. M. and Rosario, M. V. (2011). From bouncy legs to poisoned arrows: elastic movements in invertebrates. *J. Exp. Biol.* **214**, 1973-1980. doi:10.1242/jeb.038596

Proske, U. and Morgan, D. L. (1987). Tendon stiffness: methods of measurement and significance for the control of movement. A review. *J. Biomech.* **20**, 75-82. doi:10.1016/0021-9290(87)90269-7

Richards, C. T. and Sawicki, G. S. (2012). Elastic recoil can either amplify or attenuate muscle-tendon power, depending on inertial vs. fluid dynamic loading. *J. Theor. Biol.* **313**, 68-78. doi:10.1016/j.jtbi.2012.07.033

Roberts, T. J. and Azizi, E. (2011). Flexible mechanisms: the diverse roles of biological springs in vertebrate movement. *J. Exp. Biol.* **214**, 353-361. doi:10.1242/jeb.038588

Roberts, T. J. and Hoppeler, H. H. (2016). Contribution of elastic tissues to the mechanics and energetics of muscle function during movement. *J. Exp. Biol.* **219**, 266-275. doi:10.1242/jeb.124446

Roberts, T. J. and Marsh, R. L. (2003). Probing the limits to muscle-powered accelerations: lessons from jumping bullfrogs. *J. Exp. Biol.* **206**, 2567-2580. doi:10.1242/jeb.00452

Robertson, B. D. and Sawicki, G. S. (2014). Exploiting elasticity: modeling the influence of neural control on mechanics and energetics of ankle muscle-tendons during human hopping. *J. Theor. Biol.* **353**, 121-132. doi:10.1016/j.jtbi.2014.03.010

Robertson, J. W., Struthers, C. N. and Syme, D. A. (2018). Enhancement of muscle and locomotor performance by a series compliance: a mechanistic simulation study. *PLoS ONE* **13**, e0191828. doi:10.1371/journal.pone.0191828

Rosario, M. V., Sutton, G. P., Patek, S. N. and Sawicki, G. S. (2016). Muscle–spring dynamics in time-limited, elastic movements. *Proc. R. Soc. B* **283**, 20161561. doi:10.1098/rspb.2016.1561

Rospars, J.-P. and Meyer-Vernet, N. (2016). Force per cross-sectional area from molecules to muscles: a general property of biological motors. *R. Soc. Open Sci.* **3**, 160313. doi:10.1098/rsos.160313

Rubenson, J. and Marsh, R. L. (2009). Mechanical efficiency of limb swing during walking and running in guinea fowl (*Numida meleagris*). *J. Appl. Physiol.* **106**, 1618-1630. doi:10.1152/japplphysiol.91115.2008

Rubenson, J., Henry, H. T., Dimoulas, P. M. and Marsh, R. L. (2006). The cost of running uphill: linking organismal and muscle energy use in guinea fowl (*Numida meleagris*). *J. Exp. Biol.* **209**, 2395-2408. doi:10.1242/jeb.02310

Salzano, M. (2020). Musculoskeletal plasticity in response to loading history during growth. PhD thesis. The Pennsylvania State University.

Salzano, M. Q., Cox, S. M., Piazza, S. J. and Rubenson, J. (2018). American Society of Biomechanics Journal of Biomechanics Award 2017: high-acceleration training during growth increases optimal muscle fascicle lengths in an avian bipedal model. *J. Biomech.* **80**, 1-7. doi:10.1016/j.jbiomech.2018.09.001

Sawicki, G. S., Robertson, B. D., Azizi, E. and Roberts, T. J. (2015). Timing matters: tuning the mechanics of a muscle-tendon unit by adjusting stimulation phase during cyclic contractions. *J. Exp. Biol.* **218**, 3150-3159. doi:10.1242/jeb.121673

Scovil, C. Y. and Ronsky, J. L. (2006). Sensitivity of a Hill-based muscle model to perturbations in model parameters. *J. Biomech.* **39**, 2055-2063. doi:10.1016/j.jbiomech.2005.06.005

Seth, A., Hicks, J. L., Uchida, T. K., Habib, A., Dembia, L., Dunne, J. J., Ong, C. F., DeMers, M. S., Rajagopal, A., Millard, M. et al. (2018). OpenSim: Simulating musculoskeletal dynamics and neuromuscular control to study human and animal movement. *Comput. Biol.* **14**, e1006223. doi:10.1371/journal.pcbi.1006223

Snell-Rood, E. C. (2012). Selective processes in development: implications for the costs and benefits of phenotypic plasticity. *Integr. Comp. Biol.* **52**, 31-42. doi:10.1093/icb/ics067

Spoor, C. W. and van Leeuwen, J. L. (1992). Knee muscle moment arms from MRI and from tendon travel. *J. Biomech.* **25**, 201-206. doi:10.1016/0021-9290(92)90276-7

Sutton, G. P., Mendoza, E., Azizi, E., Longo, S. J., Olberding, J. P., Ilton, M. and Patek, S. N. (2019). Why do large animals never actuate their jumps with latch-mediated springs? Because they can jump higher without them. *Integr. Comp. Biol.* **59**, 1609-1618. doi:10.1093/icb/icz145

Venables, W. N. and Ripley, B. D. (2002). *Modern Applied Statistics with S*, 4th edn. New York: Springer-Verlag.

Wagenmakers, E.-J. and Farrell, S. (2004). AIC model selection using Akaike weights. *Psychon. Bull. Rev.* **11**, 192-196. doi:10.3758/BF03206482

Walmsley, B., Hodgson, J. A. and Burke, R. E. (1978). Forces produced by medial gastrocnemius and soleus muscles during locomotion in freely moving cats. *J. Neurophysiol.* **41**, 1203-1216. doi:10.1152/jn.1978.41.5.1203

Waugh, C. M., Blazevich, A. J., Fath, F. and Korff, T. (2012). Age-related changes in mechanical properties of the Achilles tendon. *J. Anat.* **220**, 144-155. doi:10.1111/j.1469-7580.2011.01461.x

Waugh, C. M., Korff, T., Fath, F. and Blazevich, A. J. (2014). Effects of resistance training on tendon mechanical properties and rapid force production in prepubertal children. *J. Appl. Physiol.* **117**, 257-266. doi:10.1152/japplphysiol.00325.2014

Wilson, A. M., Van den Bogert, A. J. and McGuigan, M. P. (2000). Optimization of the muscle-tendon unit for economical locomotion. In *Skeletal Muscle Mechanics: from Mechanism to Function* (ed. W. Herzog), pp. 517-547. Hoboken, NJ: John Wiley & Sons.

Wisdom, K. M., Delp, S. L. and Kuhl, E. (2015). Use it or lose it: multiscale skeletal muscle adaptation to mechanical stimuli. *Biomech. Model. Mechanobiol.* **14**, 195-215. doi:10.1007/s10237-014-0607-3

Yoxon, E. and Welsh, T. N. (2019). Rapid motor cortical plasticity can be induced by motor imagery training. *Neuropsychologia* **134**, 107206. doi:10.1016/j.neuropsychologia.2019.107206

Zajac, F. E. (1989). Muscle and tendon: properties, models, scaling, and application to biomechanics and motor control. *Crit. Rev. Biomed. Eng.* **17**, 359-411.

Zajac, F. E. (1992). How musculotendon architecture and joint geometry affect the capacity of muscles to move and exert force on objects: a review with application to arm and forearm tendon transfer design. *J. Hand Surg. Am.* **17**, 799-804. doi:10.1016/0363-5023(92)90445-U

Supplementary Materials & Methods

Estimation of tendon slack length from experimental measures

Tendon slack length was estimated from experimental measures of muscle and tendon morphology as follows. First, the maximum isometric force along the tendon was calculated from the maximum force along the fiber and the pennation angle at optimal fascicle length, θ_{OFL}, according to the equation:

$$F_{maxT} = F_{max} \cos\theta_{OFL}. \quad \text{(S1)}$$

The passive force of the muscle exerted on the tendon in the experimentally measured posture was found from the normalized passive muscle force as a function of normalized fiber length curve, $f_{np}(nFl)$ [104,105]. This was first scaled, for each muscle, by the maximum isometric force along the tendon, F_{maxT},

$$f_{muscP} = F_{maxT} f_{np}(nFl). \quad \text{(S2)}$$

By normalizing the experimentally measured average fiber length by the muscle's optimal fascicle length, we could calculate the normalized fiber length of the muscle in the fixed posture, *nFl*, allowing us to solve equation (S2) for the passive force, f_{muscP}, each muscle exerted on the tendon in the experimental posture. Since the three heads of the gastrocnemius attach to the Achilles tendon, the passive force of each muscle was calculated separately and summed. As the gastrocnemius intermedia head makes up ~10% of the total gastrocnemius muscle by volume, the passive contribution of this muscle was not experimentally determined for each bird but was estimated from values previously collected [61]. The passive force exerted by the muscle must be balanced by an

equal tendon force, thus, the summed passive muscle forces equal the passive force the tendon experienced in the experimental posture.

The MTU lengths, L_{MTU}, were measured on the fixed limbs by digitizing the three-dimensional paths of the MG and LG from their origins on the tibiotarsus and femur, respectively, to the insertion of the Achilles tendon on the hypotarsus. This approach inherently includes the aponeurosis in the overall tendon length. Digitizing was done using a digitizing arm (Microscribe 3DX, Immersion, San Jose, CA). The MTU path was described by 11 points. The linear distances along the MTU path were summed to obtain an overall MTU length. This experimentally measured MTU length, L_{MTU}, is the sum of the measured fiber length, L_M, the tendon's slack length, L_T, and length change in the tendon (tendon stretch) due to passive muscle fiber force. The length change in the tendon due to passive muscle fiber force can be described as the tendon strain, ε_T, times its tendon slack length, L_{T0}.

$$L_{MTU} = L_M + L_T + L_T\varepsilon_T \tag{S3}$$

The strain in the tendon due to the passive muscle fiber force, ε_T, was calculated using the experimentally measured tendon force-displacement curve. The tendon force-displacement curve was normalized by tendon length to generate a force-strain curve.

$$f_T = g(\varepsilon_T). \tag{S4}$$

The strain at which the tendon force is equal to the passive fiber force can then be found from the inverse of equation (S4) and the passive muscle force, f_{MP} .

$$\varepsilon_T = g^{-1}(f_{MP}). \quad \text{(S5)}$$

The tendon slack length, for each muscle, then, can be calculated from equations (S4) and (S5).

$$L_{T0} = \frac{L_{MTU} - L_M}{(1 + \varepsilon_T)} \quad \text{(S6)}$$

Development of subject specific models

To perform system level analyses, we modified the generic OpenSim guinea fowl model [61] to generate subject-specific models for each individual. First, the generic model was scaled to match the measured bone lengths and body mass for each bird and saved as distinct models. In each subject specific model, the generic LG and MG maximum isometric force, pennation angle, optimal fascicle length and tendon slack length were modified to match the experimentally measured and calculated properties.

The moment arms of the LG and MG acting at the ankle was fit to experimental values by adjusting the of the size and orientation of the cylindrical wrapping surface for the Achilles at the ankle. During the trial-and-error fitting process, the radius, translation, and rotation of the wrap surface was modified, and the resulting moment arm was compared to the experimentally collected data at 31-34 points across the experimental range with a mean moment arm normalized root mean square of the error (Figure S1A) of 0.009±0.007.

Additionally, the tendon force-strain curve was updated to match experimentally collected force-strain values. Because OpenSim scales the tendon force-strain curve by the maximum isometric force of the muscle, each tendon force-strain curve was normalized by the maximum isometric force capacity of the LG or MG, respectively. The parameters of the Millard muscle model's tendon force-

strain curve were iteratively varied for both the LG and MG and compared to the experimental curve for each individual, resulting in an average root mean square error (normalized by tendon force) over 26-31 points for each tendon force-length curve (Figure S1B) of 0.061+0.025.

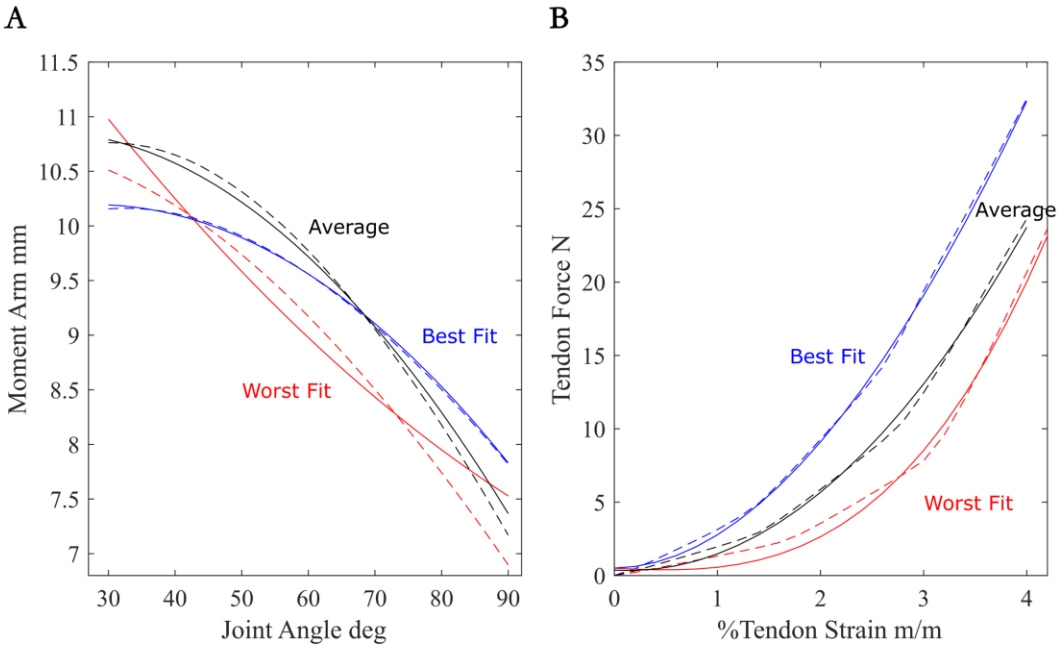

Fig. S1. Example comparisons between experimental (solid lines) and modeled (dashed lines) moment arms (A) and tendon force-strain curves (B). In each plot, experimental and modeled curves are displayed for three animals, showing the best, the average and the worst fit across individuals.